Electronic Materials Letters, Vol. 1, No. 1 (2005), pp. 11-17

Chemical Sensing with Ceramics

Hyun-Seok Hong and Chong-Ook Park*

Dept. of Materials Sci. & Engineering, Korea Advanced Institute of Science and Technology, Daejon 305-701, Korea

As industrialization has progressed, many factories have used more and more reactive and toxic chemicals, liquids, and gasses to increase competitively their productivity, which gives a severe worldwide environmental crisis. Partly in response to this development, great improvements have been made in chemical sensors over the past 30 years, especially in the area of electrochemical and surface conductive type sensors. For example, the oxygen sensor (EGO or lambda sensor), adopted for use in automobiles, has contributed to a dramatic decrease in the toxic gases CO, hydrocarbon, and NOx that are exhausted from gasoline engines. Surface conductive gas sensors, mainly made of tin oxide, have successfully served as an explosive gas detectors and alcohol checkers. In this paper, the principles of chemical detection will be presented in terms of electron/ ionic property of materials and the interface characteristics between materials. It includes electrochemical and adsorption/desorption properties of materials.

Keywords: ceramics, sensors, interfaces, amperometric sensors, potentiometric sensors

1. INTRODUCTION

Many types of gas sensors have been developed to detect chemical species in the gas phase. For instance, optical sensors detect gases based on a color change or fluorescence of a probe molecule[1]. In addition, physical sensors, such as surface-acoustic-wave devices and quartz crystal microbalances, can be used as chemical sensors when coated with polymers, self-assembled monolayers, or other chemically selective materials. Finally, there are numerous electrical sensors, which show an electrical response (e.g., resistance change or change of electromotive force) to a chemical change. Numerous electrical devices, from field effect transistors (FET)[2] to metal insulator semiconductor (MIS) diode devices[3,4] and metal oxide semiconductor capacitors[5] have been studied in connection with gas sensing behavior. The most common types of electrical sensors include potentiometric, amperometric and conductometric (or semiconductive) sensors. In this paper, the principles of surface conductive type sensors and electrochemical type sensors will be presented in section I and section II, respectively.

2. SURFACE CONDUCTIVE SENSORS

The gas molecules in an ambient can interact with (1) the bulk grain, (2) the grain boundaries or intergranular contacts and (3) the electrode/ oxide interface within oxide materials. Any of these interactions involves transfer of electrons, which brings about a change in the electrical resistance of the materials involved. Therefore, different chemical detection principles are possible, each of which utilizes the physical origins of the sensor's electrical response:

(1) bulk conduction based sensor
(2) metal/oxide junction controlled sensor
(3) surface-layer conductive sensor

2.1. Bulk conduction based sensors

When the defect species in the ceramics has a high mobility or when the temperature is high enough, the bulk phase of the ceramicscan maintain its stoichiometry in equilibrium with the gas species in the surrounding atmosphere. Because the non-stoichiometric oxide usually exhibits an electronic or a hole conductivity which is dependent on the composition of the gas component, the concentration of a gas species can be determined by measuring the bulk conductivity of the semiconducting oxides. For instance, the relationship between oxygen partial pressure and the electrical conductivity of a bulk-conduction based sensor may be represented by

$$\sigma = \sigma_o exp\left(-\frac{E_a}{kT}\right) P_{O_2}^{\pm\frac{1}{n}} \quad (1)$$

In Eq. (1), σ_o, E_a, and n are, respectively, a constant, the acti-

*Corresponding author: cops@kaist.ac.kr

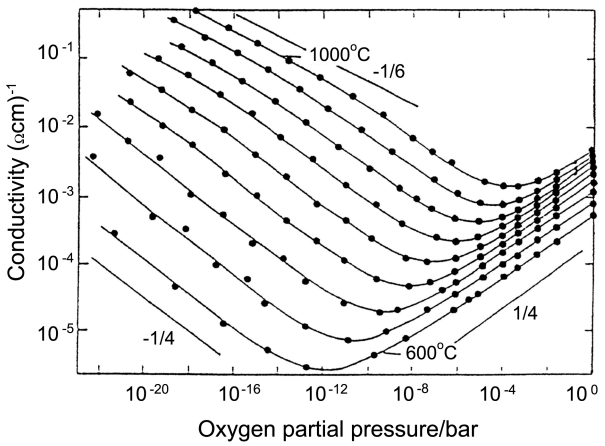

Fig. 1. The change in conductivity of $BaTiO_3$ with oxygen pressure at temperatures ranging from 600 to 1000 °C (50 °C intervals).

vation energy for the conduction, and a stoichiometric constant determined by the type of dominant bulk defect involved in the equilibrium process between oxygen and the sensor material. Positive dependence $(+1/n)$ is usually observed with high oxygen pressure in the hole-conduction region, whereas negative dependence $(-1/n)$ is usually observed at low oxygen pressure in the electron-conduction region, as shown in Fig. 1. Hence, the change in the bulk conductivity is a reflection of the equilibration between the oxygen activity in the oxide and the oxygen content (P_{O_2}) in the surrounding atmosphere. Sensors based on TiO_2[6, 7, 8], $BaTiO_3$[9], and Nb_2O_5 fall under this category.

2.2. Metal/Oxide Junction Controlled Sensors

The relative work function change upon adsorption of a gas species at the metal-oxide interface can give rise to:

(1) a change in the resistance (Schottky barrier diode)
(2) a change in the flat band voltage (MOS/MISFET devices)

In a Schottky barrier sensor[10], one of the electrode/semiconductor contacts acts as a Schottky barrier (e.g., Pd/SnO_2, Pt/TiO_2), with another electrode as an ohmic contact. The I-V characteristics of a Schottky diode are described by the thermo-electronic emission formula

$$I = A^* T^2 exp(-V_S / kT)[exp(eV / nkT) - 1] \quad (2)$$

where A^*, V_S, V, are the Richardson constant, the Schottky barrier height, and the biased voltage, respectively. The barrier height of a metal electrode/semiconductor can vary with the occupation of the surface state at a three-phase boundary (electrode/oxide/gas), which can be formed by chemisorption of oxidizing and reducing gases, such as O_2 and CO. The change in V_S leads to a change of the magnitude of the reverse saturation current and a displacement of I(V)-curve at forward bias. Hence, the partial pressure dependent variation of the interface resistance can be obtained from as can

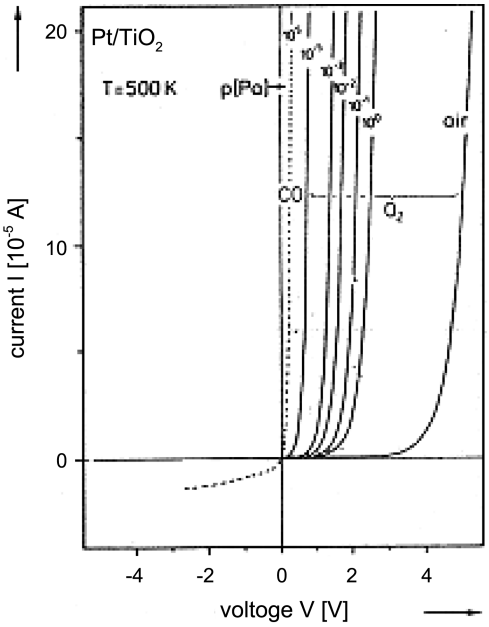

Fig. 2. I-V characteristics of Pt/TiO_2 Schottky diode in the presence of CO and O_2.

be seen in Fig. 2 for the operation modes of constant voltage mode or constant current mode. The work function change of Pd upon hydrogen adsorption has been known for more than 30 years[11]. In MOS/MISFET sensors, oxide/metal (Pd) contact is placed on Si to measure the work function change with gas adsorption via the change in the flat band voltage of semiconductor devices. In the presence of hydrogen in the ambient, hydrogen molecules are dissociated on the Pd surface into hydrogen atoms, which then diffuse through the Pd-layer to be adsorbed at the Pd-insulator interface, as shown in Fig. 3(A). At the interface, the adsorbed hydrogen atoms give rise to a dipole layer, i.e., a voltage drop, ΔV, which changes the work function of the metal at the interface. The voltage drop, ΔV can be measured from the electrical response (current or capacitance) of semiconductor devices, such as Pd-MISFET (Metal Insulator Field Effect Transistor) and Pd-MOS (Metal Oxide Capacitor). For a field effect transistor, there exists a gate threshold voltage, V_T, at which sufficient minority carriers (electrons for p-type Si) are accumulated at the semiconductor surface to yield a conducting channel. The threshold gate voltage, upon exposure to the hydrogen-containing atmosphere, is shifted negatively by ΔV, as compared to the threshold voltage, without any hydrogen-induced voltage drop at the interface, V_T^O, which is then written as

$$V_T = V_T^O - \Delta V \quad (3)$$

where $\Delta V = \Delta V_{max}[\alpha\sqrt{P_{H_2}}/(1+\alpha\sqrt{P_{H_2}})]$ is observed with α and ΔV_{max} constants (see Fig. 3(B)).

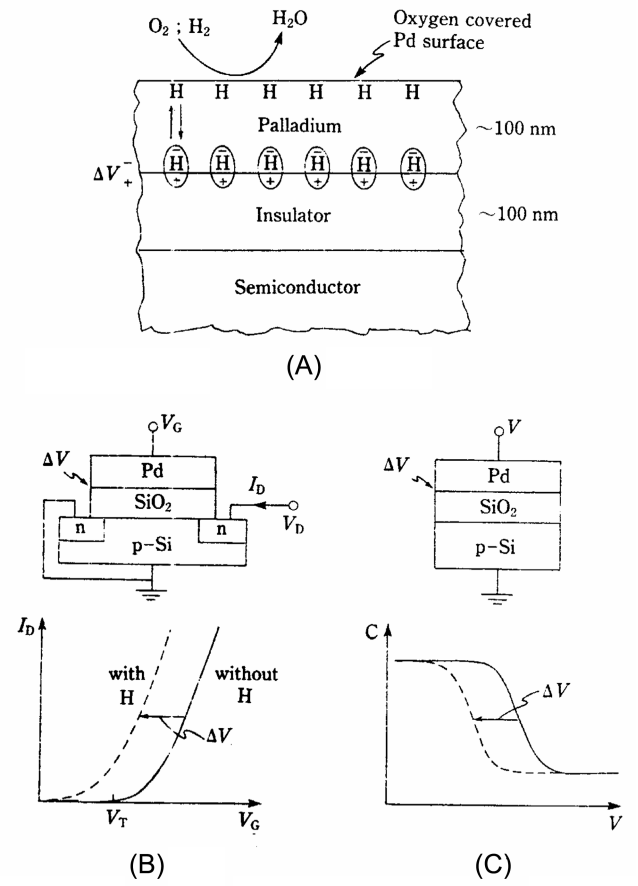

Fig. 3. (A) Schematic picture of the metal-insulator region upon chemisorption of hydrogen atoms (B) the hydrogen-induced shift of the threshold voltage characteristics of MISFET (C) the hydrogen-induced shift of the capacitance-voltage curve in MOS capacitor.

Similarly, when the high frequency (1 MHz) small signal capacitance of a MOS device, which is determined by the extent of a depletion layer at the semiconductor surface, is measured with bias voltage, it is shifted negatively along the voltage axis by ΔV, as shown in Fig. 3(C).

2.3. Surface layer conductive sensors

Surface layer conductive sensors utilize the change in the concentration of conduction electrons which occurs as a result of chemical reactions with adsorbed gas species at the surface. These reactions, chemisorption followed by a catalytic reaction, modify the defect states of the oxide's surface layer to a depth of a few microns or less. Therefore, the operating temperature should be low enough to allow sufficient surface adsorption and to slow down the bulk defect equilibration processes, yet high enough to allow catalysis reactions and charge transfer between the surface layer and the bulk interior. The working temperature of this type of sensor is usually lower than that of the bulk-conduction-based gas sensors, typically 200-500°C, depending on the base oxide and the target application.

3. ELECTROCHEMICAL SENSORS

Electrochemical sensors using solid electrolytes can be divided into three types based on the detection methods of each: equilibrium potential type, mixed-potential type, and electrochemical pumping current (amperometric type) type. Among electrochemical sensors, potentiometric gas sensors have been widely and intensively studied, because of their simple structure and high sensitivity. Three different types are used for defining potentiometric gas sensors. Type I sensors have an electrolyte from the same mobile species as that derived from the gas phase. Type II sensors do not have a mobile ion in equilibrium with the species to be sensed; rather, they have an ion related to the target gas that can travel in the solid electrolyte to allow equilibration with the atmosphere. In Type III sensors, an auxiliary phase is introduced as the sensing electrode. Type III sensors offer more practicality, in terms of designing a wide range of sensors that use different auxiliary materials and electrolytes.

3.1. Type I sensors

Oxygen sensors consist of an O^{2-}-ion conductor and two electrodes, where the chemical potential, $\mu_{O2}{}^{I}$, is known and is usually fixed by using air as the reference gas. This type of sensor can be represented by the following cell

$$(\text{Ref})\ P_{O2},\ Pt^{I} \mid ZrO_2 \mid Pt^{r},\ P_{O2}. \tag{4}$$

In (4), the Pt electrodes are electronic conductors acting as the reference and sensing electrodes. Both sides of the porous Pt electrodes enhance the oxygen diffusion and maximize three phases contact. The solid electrolyte is a gas-tight O^{2-} conductor, YSZ (Yttria-stabilized zirconia), and P_{O2} and P_{O2} (Ref) are the unknown and the reference partial pressures of the oxygen, respectively. The interfacial equilibrium reaction between the oxygen gas and the electrolyte involves electrons and ions, and this reaction occurs most readily at the three-phase junctions of the catalytic metal electrode, electrolyte, and gas phase. The electro-catalytic activity of the metal electrodes for the "redox" reaction O_2 (gas) + $4e^{-}$ $\leftrightarrow$ $2O^{2-}$ (electrolyte) is essential for selectivity, sensitivity, and short response times of the sensors. EMF is defined by the thermodynamic properties of chemical potentials at the metal/electrolyte interface and can be expressed as follows:

$$E = \frac{RT}{4F} \ln \frac{P_{O_2}}{P_{O_2}(ref)}. \tag{5}$$

Therefore, the observed potential difference is simply the difference in chemical potential of the species to be detected, which is related to the oxygen partial pressures between the "unknown" side and the reference side of the solid electrolyte.

Oxygen sensors are the most successful ceramic-based gas

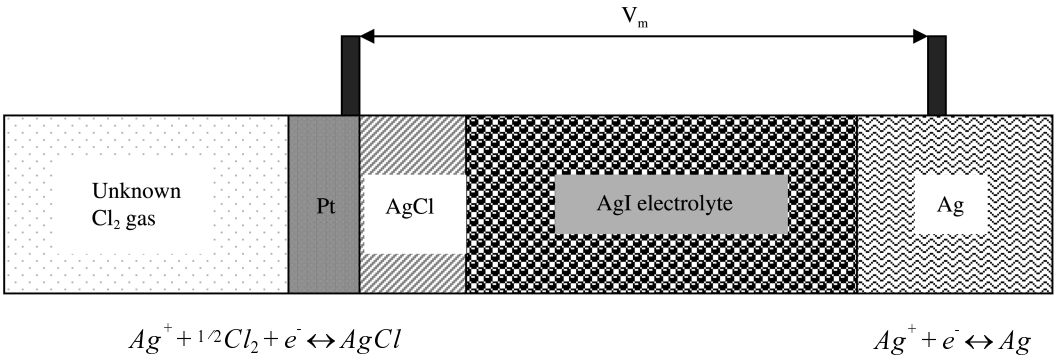

Fig. 4. Schematic set-up of a chlorine sensor using a type III arrangement.

sensors; however, this type of sensor cannot be applied to sense other gas species, because the target gas species should be the same ion as the mobile species in the ion conductor.

3.2. Type II sensors

The first type II sensor was invented by Gauthier et al. when electrochemical cells using K_2SO_4 solid electrolyte were made for the detection of SO_2. Then, Ag_2SO_4 was examined as a solid-state reference electrode, and it showed satisfactory results. The subsequent adoption of a solid reference electrode has simplified experimental procedures. The cell for CO_2 gas was fabricated on a disc (electrolyte) of K_2CO_3 in the same group[12].

$$Au \mid CO_2, O_2 \mid K_2CO_3 \mid CO_2', O_2' \mid Au \quad (6)$$

where K_2CO_3 acts as a K^+ conductor. The gaseous components interact with K_2CO_3 on the electrode (Au) to undergo an electrochemical reaction as follows.

$$2K^+ + CO_2 + 1/2O_2 + 2e = K_2CO_3 \text{ (solid)} \quad (7)$$

The EMF of the concentration cell is given by

$$E = \frac{RT}{2F} \ln \left\{ \frac{P'_{CO_2}(P'_{O_2})^{1/2}}{P_{CO_2}(P_{O_2})^{1/2}} \right\} = \frac{RT}{2F} \ln \frac{P'_{CO_2}}{P_{CO_2}} \quad (8)$$

If $P'_{O2} = P_{O2} = 0.21$ atm, a simple CO_2 concentration cell is established, enabling one to estimate P'_{CO_2} from E for known P_{CO2}. However, an electrolyte made with K_2CO_3 would not be acceptable in practice. The electrolyte should be free of pin-holes, exhibit adequate levels of ionic conductivity, and be mechanically, chemically and thermally stable. A great deal of effort has been exerted to develop better electrolyte materials, particularly for SO_2 sensors.

3.3. Type III sensors

Type II sensors, which are based on the internal equilibrium between the species to be detected and an immobile component of the electrolytes, are still restricted to using a few of the presently known fast solid ionic conductors. This limitation has prompted the development of type III sensors, which use auxiliary solid phase layers. This indirect galvanic determination method for measuring activities of mobile ion in a thin sensitive material, the so-called auxiliary phase, onto a solid electrolyte can be extended to many selective measurements. For instance, chlorine partial pressures can be determined using the combination of Ag ion conducting electrolyte and a AgCl auxiliary layer.

Under open circuit conditions and thermal equilibrium, the EMF the chemical potential of chlorine gas at the interface between the auxiliary phase and the electrolyte is given by equation (9)

$$V_m = \frac{-\Delta G^0(AgCl)}{q} + \frac{RT}{2F} \ln [P(Cl_2)] \quad (9)$$

where $\Delta G^0(AgCl)$ is the standard free energy of formation of $AgCl$, and $P(Cl_2)$ is the partial pressure of target chlorine gases It is assumed that all of the potential drop occurs at the electrolyte/electrode interface and that the chemical activity of silver and silver chloride in this equation is equal to unity.

3.4. Mixed potential sensors

When more than one electrochemical reaction is involved at the electrode, the equilibrium potential becomes a mixed potential that is generated from the competition of all reactions occurring at the electrode. For example, when a Au and Pt electrode fabricated on yttria-stabilized zirconia electrolyte is exposed to an environment containing CO, CO_2, and oxygen, as shown in Fig. 5, an oxygen reduction reaction,

$$O_2 + 4e \rightarrow 2O^{2-} \quad (10)$$

occurs at a rate that accords with the Butler-Volmer equation,

$$i_{O_2} = i^O_{O_2} exp[-4\alpha_1 F(E - E^O_{O_2})/RT] \quad (11)$$

and a corresponding carbon monoxide oxidation reaction,

$$CO + O^{2-} \rightarrow CO_2 + 2e \quad (12)$$

occurs simultaneously at a rate express as

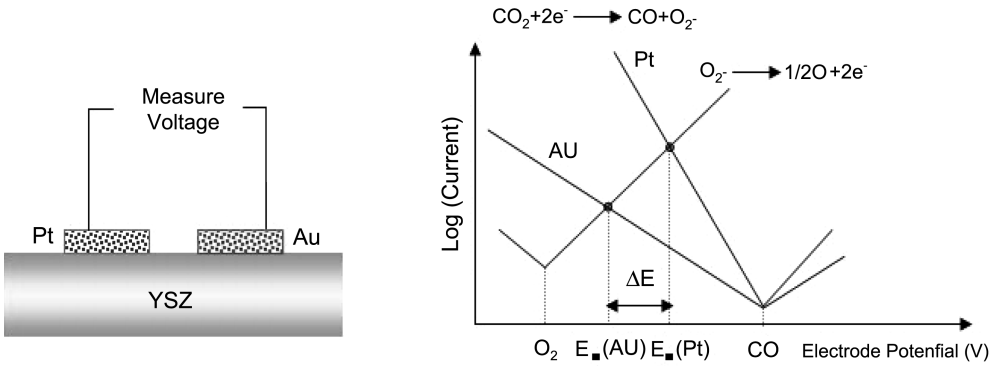

Fig. 5. Schematic structure of mixed potential sensor with its cathodic and anodic reactions.

$$i_{CO} = i_{CO}^{O} exp[2\alpha_2 F(E - E_{CO_2}^{O})/RT] \quad (13)$$

to yield a mixed potential meeting the condition, $i_{O_2} = i_{CO}$. Therefore, assuming $i_{O_2}^{O} = k_1 P_{O_2}^{m}$ and $i_{CO}^{O} = k_2 P_{CO}^{n}$, the equilibrium mixed potential becomes

$$E_{mix} = E^{O} + [RT/(4\alpha_1 + 2\alpha_2)F][m \ln P_{O_2} - n \ln P_{CO}] \quad (14)$$

where $E^{O} = \frac{RT}{F(4\alpha_1+2\alpha_2)} \ln \frac{k_2}{k_1} + \frac{2\alpha_1 E_{O_2}^{O} + \alpha_2 E_{CO}^{O}}{2\alpha_1 + \alpha_2}$. For a constant oxygen partial pressure, the equilibrium mixed potential becomes logarithmic dependence on P_{CO} expressed as

$$E = E^{O} + [\beta RT/F] \ln P_{CO} \quad (15)$$

where E^{O} and β are constants.

However, if E_{mix} is close to equilibrium oxygen potential,[13] such that the oxygen reduction reactions occur at a low overpotential and carbon monoxide oxidation reactions occur at a high overpotential, then the oxygen reduction kinetics may be represented by Tafel-type equation, a low overpotential approximation of the Butler-Volmer equation,

$$i_{O_2} = i_{O_2}^{O} 4\alpha_1 F(E - E_{O_2}^{O})/RT \quad (16)$$

In addition, the oxidation reaction kinetics may be represented by the mass transport limited process due to a high overpotential,

$$i_{CO} = -2FAD_{CO}\frac{P_{CO}}{RT\delta} \quad (17)$$

where A and δ correspond to the electrode area and the depth of the stagnant boundary layer, respectively. Combining Eq. (16) with (17) for $i_{O_2} = i_{CO}$ yields

$$E_{mix} = E_{O_2}^{O} - \frac{AD_{CO}}{2i_{O_2}^{O}\alpha_i\delta} P_{CO} \quad (18)$$

which provides the linear relationship between the CO concentration and the mixed potential.

Garzon *et al.*[14] observed the linear dependence of a mixed potential on the concentration of reducing gases from the cell $Pt|Ce_{0.8}Gd_{0.2}O_{1.9}|Au$, as illustrated in Fig. 6.

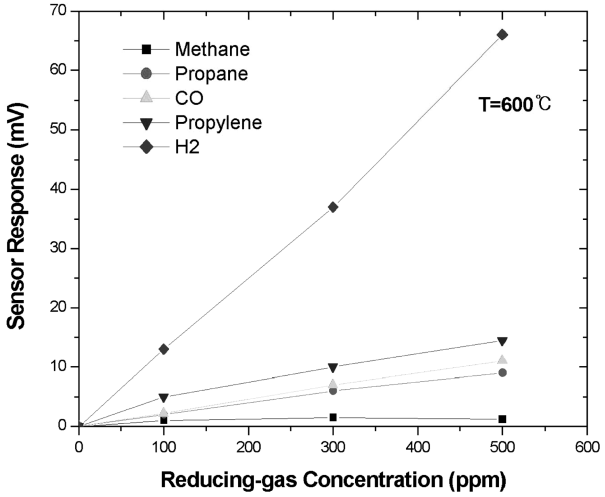

Fig. 6. Mixed potential obtained from the cell, $Pt|Ce_{0.8}Gd_{0.2}O_{1.9}|Au$, exposed to various reducing gases at 600 °C.

3.5. Amperometric Sensors

The basic configuration of the amperometric electrochemical sensor, sometimes-called a limiting-current-type sensor, is shown in Fig. 7(a). An amperometric sensor consists of a restricted volume of zirconia cell with a pumping electrode inside and a small aperture for a diffusion hole. When the electrode inside the cell is negatively biased, the oxygen atoms will be ionized at the cathode into oxygen ions, which are then pumped away to the anode outside the cell.

Depending on the ratio of the pumping rate to the diffusion flux of oxygen through the hole, limiting-current-type sensor shows three regions of I-V characteristics, as shown in Fig. 7(b). The biased voltage, V, is expressed as

$$V = iR + RT/4F \ln P_{O_2}[(ambient)/P_{O_2}(cathode)] \quad (19)$$

At a low voltage (region I) where the pumping rate is less than the diffusion flux, i.e., $P_{O_2}(ambient) = P_{O_2}(cathode)$, the current increases linearly with the biased voltage as $V = iR$. As the pumping rate increases to higher thanthe diffusion flux of oxygen through the aperture, the current

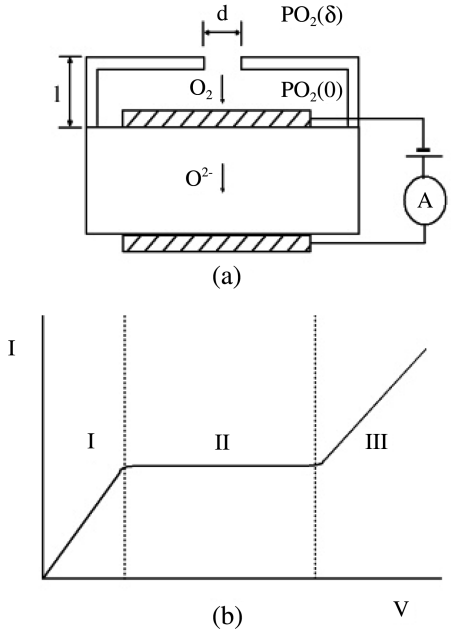

Fig. 7. Schematic structure of amperometric sensor and its typical response.

reaches a steady state (region II), which is determined by the rate of oxygen arrival from the ambient to the electrode and is expressed as

$$J_{O_2} = i/4F = D_{O_2}[C_{O_2}(\delta) - C_{O_2}(0)]/\delta \approx [D_{O_2}P_{O_2}]/[RT\delta] \quad (20)$$

In Eq. (20), δ corresponds to the effective diffusion length for oxygen, and $c_{O_2} = P_{O_2}/RT$ has been assumed . If the biased voltage is large enough (normally 0.5 – 1.5 V), then the oxygen partial pressure at the cathode will decrease to nearly zero, $c_{O_2} \approx 0$, which provides the last term in Eq. (20). Hence, the pumping current at a steady state depends linearly on the oxygen partial pressure in the ambient, and this is the reason why it is sometimes called a proportional oxygen gauge adopted for the lean burn engines in automobiles. However, it is to be noted from Eq. (19) that the increase in voltage is compensated by the decrease in oxygen pressure at the cathode for a constant limiting current. As the biased voltage increases to region III, where the oxygen partial pressure becomes lower than 10^{-33} atm, electronic conduction occurs to provide a further increase in current by the electronic conduction resulting from the decomposition reaction, $O_O^{\times} \rightarrow V_O^{\cdot\cdot} + 1/2O_2 + 2e$. In practice, the limiting-current-type sensor is operated in region II, where a steady state current can be obtained.

4. FUTURE TRENDS

The fundamentals of various kinds of chemical sensors have been discussed. Such fundamentals have contributed to the tremendous advancement in chemical sensor technology in the world, as exemplified by a variety of important applications in car industries, plant facilities, safety appliances, environmental protections, and medical appliances.

Currently, the demand for more sophisticated sensors is increasing in response to quality of life issues, global environmental issues, biomedical diagnosis concerns, and other concerns.

Another active area of gas sensor research is the use of pattern-recognition techniques to generate selectivity from sensors that may otherwise appear non-selective[15]. Some of these pattern-recognition approaches are as simple as monitoring the sensor response over a range of temperatures, while others involve the use of artificial neural networks. However, in real-life applications, the objective of a given pattern recognition approach may be difficult to achieve, as a sensor array's functionality relies not only on the right combination or integration of different sensors, but also on the stability of individual sensors. Any change or drift in one of the sensors requires a complete recalibration or reprogramming of the pattern recognition components. In other words, potential applications of a sensor array system are still going to be determined by the availability of stable and reliable individual sensors.

ACKNOWLEDGEMENTS

The authors are grateful for the financial support from the Core Environmental Technology Development Project for Next Generation by KIEST (Korea Institute of Environmental Science and Technology) and Center for Ultramicrochemical Process Systems sponsored by KOSEF (Korea Science and Engineering Foundation).

REFERENCES

1. M. Ross, R. Goodwin, and R. Watkins, 2000 and 2010 Passenger Cars (1996).
2. E. M. Logothetis, *Chemical Sensor Technology* **3**, 89 (1991).
3. O. W. Bynum, D. R. Sheridan, and J. A. White, GRI Report 92/0373, (1992).
4. H. N. McMurray and J. Albadran, *MRS Bulletin* **34**, 55 (1999).
5. M. Leu, T. Doll, B. Flietner, J. Lechner, and I. Eisele, *Sens. Actuators B* **18-19**, 678 (1994).
6. Y. Gurbuz, W. P. Kang, J. L. Davidson, and D. V. Kerns, *Sens. Actuators B* **56**, 151 (1999).
7. W. P. Kang and C. K. Kim, *Sens. Actuators B* **13-14**, 682 (1993).
8. A. Samman, S. Gebremariam, L. Rimai, X. Zhang, J. Hangas, and G. W. Auner, *Sens. Actuators B* **63**, 91 (2000).
9. O. K. Tan, X. F. Chen, and W. Chu, *J. Mater, Sci.* **21**, 4353-

4363 (2003).
10. L. D. Birkefeld, A. M. Azad, and S. A. Akbar, Carbon Monoxide and Hydrogen Detection by Anatase Modification of Titanium Dioxide, *J. Am. Ceram. Soc.* **75**, 2964 (1992).
11. J. R. Stetter, *J. Coll. Inter. Sci.* **65**, 432 (1977).
12. M. Gauthier and A. Chamberland, *J. Electrochem. Soc*. **124**, 1579 (1977).
13. W. J. Fleming, *J. Electrochem. Soc.* **124**, 21 (1977).
14. R. Mukundan, E. Brosha, D. R. Brown, and F. H. Garzon, *Proceeding of the 195th Electrochemical Society Meeting on Solid State Ionic Devices Symposium* (eds., E. D. Wachsman, M. -L. Liu, J. R. Akridge, and N. Yamazoe), p. 360-373, Seatle, WA (1999).
15. J. W. Gardner and P. N. Bartlett (eds), *Sensors and sensory systems for an electronic nose. NATO ASI Series E: Applied Science,* Vol. 212. Kluwer, Dorderecht (1992).